CORA Cork Open Research Archive
Cartlann Taighde Oscailte Chorcaí

Title	First responders occupancy, activity and vital signs monitoring - SAFESENS
Authors	O'Flynn, Brendan;Brahmi, Imane;Oudenhoven, Jos;Nackaerts, Axel;Pereira, Eduardo;Agrawal, Piyush;Fuchs, Tino;Braun, Tanja;Lang, Klaus-Dieter;Dils, Christian;Walsh, Michael
Publication date	2018
Original Citation	O'Flynn, B., Brahmi, I., Oudenhoven, J., Nackaerts, A., Pereira, E., Agrawal, P., Fuchs, T., Braun, T., Lang, K.-D., Dils, C. and Walsh, M. (2018) 'First responders occupancy, activity and vital signs monitoring - SAFESENS', International Journal on Advances in Networks and Services, 11(1-2), pp. 22-32. Available at: http://www.iariajournals.org/networks_and_services/netser_v11_n12_2018_paged.pdf (Accessed: 21 January 2019)
Type of publication	Article (peer-reviewed)
Link to publisher's version	http://www.iariajournals.org/networks_and_services/, http://www.iariajournals.org/networks_and_services/netser_v11_n12_2018_paged.pdf
Rights	© 2018, the Authors. Published by International Academy, Research and Industry Association (IARIA). This article is made available under a Creative Commons Attribution-Non Commercial-Share Alike license. - https://creativecommons.org/licenses/by-nc-sa/2.5/
Download date	2026-11-15 00:42:30
Item downloaded from	https://hdl.handle.net/10468/7323

UCC
University College Cork, Ireland
Coláiste na hOllscoile Corcaigh

First Responders Occupancy, Activity and Vital Signs Monitoring - SAFESENS

Brendan O'Flynn, Michael Walsh, Imane Horiya Brahmi
Tyndall National Institute
University College Cork
Cork, Ireland
brendan.oflynn@tyndall.ie
michael.walsh@tyndall.ie
imane.brahmi@tyndall.ie

Jos Oudenhoven
Holst Centre-imec
High Tech Campus 31
Eindhoven, The Netherlands
jos.oudenhoven@imec-nl.nl

Axel Nackaerts
NXP Semiconductors Belgium
Interleuvenlaan 80
Leuven, Belgium
axel.nackaerts@nxp.com

Eduardo Pereira, Piyush Agrawal
UTRC: United Technologies Research Center
4th Floor, Penrose Wharf Business Centre
Penrose Quay, Cork, Ireland
pereirem@utrc.utc.com
agrawaP@utrc.utc.com

Tino Fuchs
Robert Bosch GmbH
Renningen, 70465 Stuttgart, Germany
Tino.Fuchs2@de.bosch.com

Tanja Braun, Klaus-Dieter Lang
Technical University Berlin
Berlin, Germany
tanja.braun@tu-berlin.de
k.lang@tu-berlin.de

Christian Dils
Fraunhofer IZM
Berlin, Germany
christian.dils@izm.fraunhofer.de

Abstract **- This paper describes the development and implementation of the SAFESENS (Sensor Technologies for Enhanced Safety and Security of Buildings and its Occupants) location tracking and first responder monitoring demonstrator. An international research collaboration has developed a state-of-the-art wireless indoor location tracking system for first responders, focused initially on fire fighter monitoring. Integrating multiple gas sensors and presence detection technologies with building safety sensors and personal monitors has resulted in more accurate and reliable fire and occupancy detection information. This is invaluable to firefighters in carrying out their duties in hostile environments. This demonstration system is capable of tracking occupancy levels in an indoor environment as well as the specific location of fire fighters within those buildings, using a multi-sensor hybrid tracking system. This ultra-wideband indoor tracking system is one of the first of its' kind to provide indoor localization capability to sub meter accuracies with combined Bluetooth low energy capability for low power communications and additional inertial, temperature and pressure sensors. This facilitates increased precision in accuracy detection through data fusion, as well as the capability to communicate directly with smartphones and the cloud, without the need for additional gateway support. Glove based, wearable technology has been developed to monitor the vital signs of the first responder and provide this data in real time. The helmet mounted, wearable technology will also incorporate novel electrochemical sensors which have been developed to be able to monitor the presence of dangerous gases in the vicinity of the firefighter and again to provide this information in real time to the fire fighter controller. A SAFESENS demonstrator is currently deployed in Tyndall and is providing real time occupancy levels of the different areas in the building, as well as the capability to track the location of the first responders, their health and the presence of explosive gases in their vicinity. This paper describes the system building blocks and results obtained from the first responder tracking system demonstrator depicted.**

Keywords - Gas Sensors; Body Area Networks; Activity Tracking; Vital Signs Monitoring; Occupancy Detection.

I. INTRODUCTION

The SAFESENS indoor first responder localization and activity monitoring system [1], is designed based on the latest available sensor technologies. It incorporates several solutions to an emergency situation including people counting for an efficient rescue operation and first responder location tracking [2]. To meet the most demanding application needs, we have designed a sensor board along with the wireless network infrastructure which is capable of delivering the next generation of safety devices. The objectives of the Tyndall National Institute (TNI) in this project, is to develop a wearable [3] indoor localization and activity monitoring system for first responders during emergency situations. In parallel, novel explosive or flammable gas sensor technologies and physiological health monitoring systems are being integrated into the fire fighters' apparel to monitor their health and well-being as they are tracked through the system as in Figure 1.

This publication describes the indoor localization platform of the SAFESENS project, the vital signs monitoring and flammable gas sensing and presents results from the SAFESENS deployment. Section II of this publication discusses the state of the art in first responder systems, Section III presents the system architecture for the SAFESENS system, Section IV presents the location tracking system, Section V presents the Vital Signs monitoring system, Section VI describes the explosive/flammable gas sensing system, Section VII describes the occupancy monitoring system, and Section VIII describes the test results obtained from each of these building blocks. Section IX concludes the work.

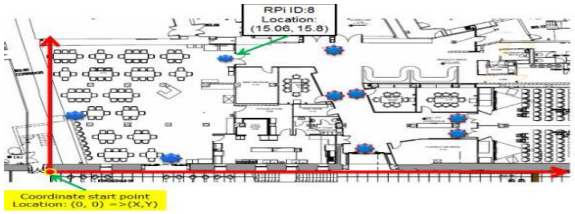


Figure 1. Deployment Area – Tyndall National Institute UCC.

2018, © Copyright by authors, Published under agreement with IARIA - www.iaria.org

II. State of the Art in First Responder Systems

At present, several projects have been reported on personal safety monitors for first responders. These are mainly directed towards vital signs monitoring and indoor localization. Even though there are not many systems available on the market yet, several research projects have resulted in demonstrators in the form of wearable systems.

An example of a vital signs monitoring system is the Equivital EQ02, a body worn system that can track the vital signs via ECG (electrocardiography), respiratory rate, skin temperature, accelerometer and body position [4]. Also, other projects are focused on vital sign monitoring. For example, the Phaser project (Phaser: Physiological Health Assessment System for Emergency Responders). In this project, the pulse, body temperature and blood pressure are measured [5].

An example of a truly wearable system that was developed is the WASP (Wearable Advanced Sensor Platform). This platform was developed at Worcester Polytechnic Institute and industrialized by Globe Manufacturing Company. It has the form of a T-shirt, in which vital sign sensors are positioned around the chest. The system integrates a Zephyr BioHarness and a Pebble Smart Watch for physiological monitoring, tracking and communications [7].

Another aspect that is important for personal safety monitors are gas concentrations of the environment. There are already several portable (hand-held) systems available on the market that can fulfil this task. These devices are, in general, small devices with a display at which the measured concentrations can be read. Mostly, these devices do not incorporate wireless communication. Examples of portable gas sensors are the devices manufactured by Dräger [8], Scott Safety [9], ION Science [10], RKI instruments [11] and RAE systems [12]. In general, devices are available containing sensors for one up to four gases integrated in a single housing. These sensors make use of various sensing methods, for example: electrochemical cells, photo-ionization detection, metal oxides et cetera. These types of sensors are available for many different gases, including CO, O_2, H_2S, NH_3, Cl_2, PH_3, SO_2, and volatile organic compounds.

Tracking rescue personnel within buildings in emergency situations and providing reliable communications among them, is a problem which has attracted considerable attention in recent years. A number of solutions (products/prototypes) have already been proposed in literature or on the market. Examples of such systems are:

Precision Personnel Locator (PPL) of the Worcester Polytechnic Institute (Locator and Health Status Display), based on inertial sensors and OFDM. Position/Location Tracking and Communications Software Defined Radio (POSCOMM) [13] from NAVSYS, based on GPS and TOA pseudolite observations implemented with SDR technology. NAViSEER [14] from SEER Technology, based on inertial sensors, GPS and cellular/RF communication. Harris GR-100 [15] from Harris Corporation, based on inertial sensors, GPS and on-scene tactical radio networks for communication. Personnel Navigation, Locating and Tracking [16] from ENSCO, based on inertial sensors, GPS, compass, and 2.4 GHz RF Ranging. TRX Sentrix Systems [17], based on inertial sensors, GPS, compass, TOA RF Ranging, barometer, and light sensor. GLANSER [18] from Honeywell, TRX Systems, and Argon ST, based on inertial sensors, GPS, compass, 900 MHz Ranging, barometer, Doppler Radar + Map correction. FLARE [19] from Q-Track, based on customized active RFID technology. Q-Track's FLARE succeeded in a realistic trial held at the 5th Workshop on Precision Indoor Personnel Location and Tracking for Emergency Responders at Worcester Polytechnic Institute, but has not been released as an ongoing product The EUROPCOM [20] project involving Thales UK, Delft University of Technology, Graz University of Technology, IMST GmbH, based on UWB and GPS.

III. System Architecture

In order to ensure that real world problems were being addressed within the project, engagement with end users was undertaken from an early stage of the SAFESENS project. So as to collect feedback from the stakeholder and end-user community, an "End-user" workshop was organized in conjunction with the Security Essen Fair in Essen, September 2014. A "First responder workshop" was organized with the fire brigade of Murcia and its regions in February 2015, and an additional End-user questionnaire was launched on SurveyMonkey and feedback collected from various stakeholders. Based on the feedback from these stakeholders, an appropriate system architecture and demonstrator was defined incorporating the requirements around sensors to be developed and integrated in the first responder body area network. This also captured issues such as the preferred location of the sensors – (on the strap of the air tank, as requested by fire fighters), as well as the appropriate communications and localization mechanisms and infrastructure definition.

As part of the user need exploration, it was identified that presence data and occupancy levels could be very valuable to first responders so they can plan their rescue team and evacuation plans. This could result in reduced loss of lives (in both rescuer and rescued). The Murcia firefighters are currently using a variety of communications systems: A microphone is integrated into a mask and is connected through a wire to the mask with a push to talk system - TETRA [21].

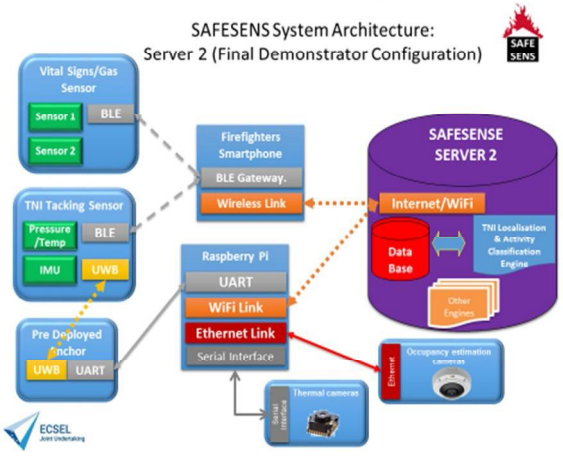


Figure 2. SAFESENS Demonstrator System Architecture.

2018, © Copyright by authors, Published under agreement with IARIA - www.iaria.org

The SAFESENS system architecture developed to meet the user requirements demonstrator is shown in Figure 2. There are 8 separate system building blocks comprising the SAFESENS system: the server, mobile gateway (fire fighter's smartphone), Ultra-wide band (UWB) localization [22] Access Points, Raspberry Pi, occupancy detection camera, firefighter tracking node, the Vital Signs monitoring system and the explosive gas detector. With the implemented sensor platform, we are able to collect real time data for research and analysis.

The smartphone carried by the firefighter acts as the integration system, harvesting the sensory data sets from the firefighters' apparel and sending it to the server for processing, running python based analytic/localization engines and to facilitate visualisation of the data streams.

IV. Location and Activity Tracking

A significant number of firefighters are injured every year in the line of duty [23]. Tracking firefighters while deployed in dangerous environments is critical to mitigate risk to the personnel.

A. Introduction to First Responder Activity Monitoring

In large buildings, there is often a requirement to enter and deal with fires from multiple directions in order to prevent the fire from spreading. Line of sight is often obscured with smoke and debris [24] and there is also the possibility that parts of the structure may be unstable and subject to collapse. Information relating to the position and activity status of the firefighter is therefore critical in helping the subject to navigate the environment, and to enable safe extraction in the Non Line of Sight (NLOS) case [25]. This information is also valuable in search and rescue situations, to enable more optimal and efficient use of personnel on the ground.

B. SAFESENS Localization Technologies

The SAFESENS project has developed a Personnel Safety Monitor, the purpose of which is to become a tool for first responders and their commanders to help with indoor navigation in obscured conditions in a fire situation, and to give an assessment of the safety of the first responder. For indoor localization, a system is required that is independent of the existing building infrastructure, since this infrastructure may become unreliable or damaged in a fire situation. SAFESENS has integrated into the platform a hybrid inertial, positional and navigation module illustrated in Figure 3.

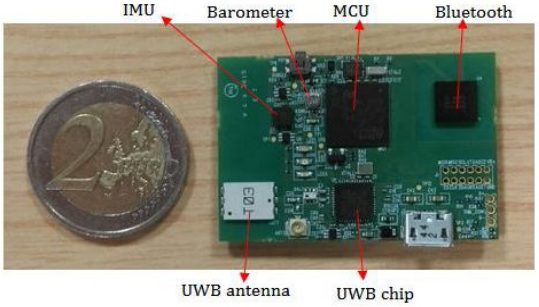


Figure 3. Hybrid Inertial, Positional and Navigation Module

The modules' onboard sensors are capable of providing information to enable activity to be classified and position to be determined in deployment scenarios where there is little supporting existing wireless infrastructure in place.

The hybrid inertial, positional and navigation module is designed to be worn by each first responder attached to the straps of their SCBA (Self-Contained Breathing Apparatus). The hardware comprises of inertial and magnetic sensors (accelerometer, gyro, and magnetometer), a barometer, a temperature and humidity sensor, an UWB ranging transceiver and a Bluetooth Low-Energy (BLE) transceiver. The module communicates sensor data to a smartphone carried by the firefighter employing BLE, which in turn transmits data to a central server for processing. Ranging data is given by the UWB transceiver, which measures the range between the worn module and the nearby anchors to track the firefighter [26]. Anchors can be stationary units deployed as part of the exercise or alternatively, other modules worn by accompanying firefighters. The firefighter's position and current activity is calculated on the central server as illustrated in the system architecture diagram in Figure 2.

V. Vital Signs Monitoring

The integration of vital physiological measurements could help commanders to better predict the firefighter's or other first responder's health condition while performing critical tasks or in harsh environments.

A. SAFESENS Vital Signs Monitoring

An important vital parameter is the heart rate which can be calculated and monitored from either Electrocardiography (ECG) or Photo Plethysmography (PPG) signals. Fabric-based, dry electrodes have been intensively investigated for wearable ECG measurements but still need complex algorithms to eliminate motion [27]. In the SAFESENS project, we are focusing on reflective PPG measurements based on optical sensors which are more precise in mobile conditions when the sensor is attached to the skin in an appropriate way [28]. The skin volume changes due to blood pressure variations and thus correlates to the heart rate. An algorithm first removes the impact of ambient light leakage and motion artefacts, and determines the pulse period. By measuring the PPG at multiple wavelengths, it is possible to detect changes in blood composition. For instance, the change from hæmoglobin (Hb) to oxygenated hæmoglobin (HbO_2) can be detected by a relative change in red and infrared absorption [29].

B. Integrating Electronics into a Firefighter Glove

The SAFESENS firefighter glove demonstrator consists of a selected multi-chip package featuring 3 emitters (green, red, infrared) and one detector in a small package (4.7mm x 2.5mm x 0.9mm), enabling the measurement of the heart rate and pulse oximetry. The chip is integrated into an EN 659:2003 + A1:2008 certified, professional leather glove for the fire brigade and features the highest industrial cut resistance and fire blocking levels. Developed in the form factor of a sensorised ring, the sensor position is designed to be placed in an unobtrusive body area: the base of the left

2018, © Copyright by authors, Published under agreement with IARIA - www.iaria.org

hands' index finger (assuming right-handed fireman), allowing the user to touch objects without feeling the electronics. In order to contact the sensor and skin, a small hole was pierced into the glove. The controller unit is placed in a little pocket at the edge of the cuff at a distance of 250mm to the sensor.

Electronic systems, when integrated into clothing, experience dynamic tensile loads in three directions. Conventional rigid substrates like FR4 cannot meet this requirement. Even flexible substrates made of PI, PET or PEN are not suitable because they are designed for bending and folding conductor tracks around only a single axis. Therefore, the development of new materials and technologies for the realization of stretchable electronic systems are of high interest and research is increasing for about a decade. It is expected that those polymer- or textile-based technologies will primarily find use in medical electronics, robotics and wearables in future.

For the integration of the optical chip into the glove, we are using a stretchable substrate made of thermoplastic polyurethane (TPU). The used elastomer film with a thickness of 100µm can be stretched up to 500% and has a melting temperature of 165°C. On the TPU carrier material, a 17µm copper (Cu) foil is laminated. It has been suggested by M. Gonzales et al. to achieve stretchability into Cu material simply by an undulating design of the Cu tracks. In the FEM simulation, the best mechanical performance was predicted for a horseshoe like meandering structure [30]. Such boards can be stretched (once) up to 300% before fracture of the Cu lines occurs. For repeated stretch cycles, elongations with a few percent can be conducted several ten thousands of times, before fatigue fractures occur in the copper. Electronic components are assembled after local application of a solder mask and surface finish for solderability. The electronic interconnection is established using a low temperature solder alloy (SnBi, Tm=142 °C). For protection and enhanced system robustness, all components are subsequently encapsulated within a polyurethane capping [31].

Because the electronic components and copper tracks are embedded into the thermoplastic matrix, the system can be easily integrated onto textiles by a simple lamination process [32]. For the integration of the SAFESENS heart rate monitor, the system was laminated onto a fire-retardant nonwoven and finally sewn into the inner layer of the firefighter glove.



Figure 4. SAFESENS Firefighter Glove Demonstrator: X-ray images of the Textile-integrated Stretchable Electronic System

C. Signal Acquisition and Processing

The sensor front-end is a single integrated circuit containing all necessary analog circuits to drive the LEDs and to determine the photocurrent from the photodiode, and a full-featured ARM M0+ microcontroller core to run the algorithms for the heart rate and the blood oxygenation calculations. A second IC contains the wireless transceiver to connect the sensor to a Personal Area Network. In the demonstrator, the sensor communicates over a BLE link, with a protocol fully compatible with the indoor localization module. The PPG sensor can either transmit continuous measurements or act on user-selectable alarm thresholds.

VI. FLAMMABLE GAS SENSING

In the process of a burning building, a flashover is a much feared stage. A flashover occurs at the moment when temperatures are so high that any flammable materials and gases present will spontaneously combust.

A. Introduction to Flammable Gas Detection

. Flammable gases pose a particular risk during flashovers. Before a flashover, the high temperature results in partial decomposition and release of flammable gases. When sufficient oxygen is present, or is introduced due to opening or breaking of doors and windows, spontaneous combustion will occur that will accelerate the propagation of fire and pose a severe safety threat to the fire fighters. To be aware of the flashover risks, it is advantageous to be able to detect the presence of flammable gases.

B. SAFESENS Technology Developed for Gas Detection

In the SAFESENS project, it is envisioned that the first responders bring gas sensors to the scene that are integrated in their current equipment. The helmet was chosen as the most suitable location for the gas sensor, since it is a rigid structure that is in close contact with the surrounding atmosphere.

Hydrogen (H_2) may be detected using a Pd-Ni alloy as a thin film deposited onto a silicon wafer substrate, which changes its electrical resistance in the presence of H_2, which can be electrically transduced.

Methane may be detected using an amperometric electrochemical sensor. In this type of electrochemical sensor, a chemical reaction takes place that involves electron transfer in the chemical reaction pathway. By leading these electrons through an external circuit, an accurate current measurement can be performed, that is directly related to the amount of gas that is reacting. The amount of reacting gas is in its turn linearly related to the amount of gas in the surrounding atmosphere. In the SAFESENS project, a thin film methane sensor was developed that uses an ionic liquid as the electrolyte. Previously, it was reported that such sensors may be applied to detect ethylene [33], and ammonia [34].

The H_2 sensor is based on an alloy system described in [35]. Instead of using a van der Pauw structure, a Wheatstone half-bridge was realized, which gives first order temperature compensation. The Pd-Ni film was deposited using a co-sputter process from pure Pd and Ni sputter targets. Film thickness was in the range of 100nm.

2018, © Copyright by authors, Published under agreement with IARIA - www.iaria.org

The methane sensor is based on the ammonia sensor that was previously described [34]. In brief, a system of interdigitated platinum micro electrodes is made on a silicon substrate. The third electrode is a gold electrode that meanders between these interdigitated electrode, and serves as a pseudo reference electrode. On top of these electrodes, a thin film of an ionic liquid is deposited, to obtain an electrochemical cell sensitive to methane. The chosen ionic liquid is $[C_4mpy][NTf_2]$, of which it is known that this system results in an electrochemical cell that is sensitive to methane [36].

VII. Occupancy Monitoring

Occupancy estimation uses the readings from a sensor network to extract more contextual information of the building usage.

A. Introduction to Occupancy Monitoring Systems

Occupancy sensors can enable the idea of smart buildings in different ways by: i) improving the comfort of the occupants by controlling lights, temperature, and humidity based on occupancy; ii) reducing energy costs by controlling lights and HVAC equipment based on occupancy; iii) improving the convenience; iv) providing real-time occupancy in fire events. It can also offer technical advantages in a two-fold way: i) cost-benefit trade-off analysis for the selection of sensors and their placement; ii) complementary sensor measurements based on models of building usage.

B. SAFESENS Technologies for Occupancy Detection

The challenge of real-time occupancy estimation is to determine the number of people in different areas of a building over time. Under such operational settings, an estimation variance, along with a confidence level, should be provided within a short delay and fast update rate.

Due to the high deployment cost and large errors that people counting sensors suffer from, measuring occupancy throughout a building from sensors alone is not sufficiently accurate. Indeed, data collection from sensors is not perfect, and it is assumed that each sensor is subject to noise and environment clutter. Also, if sparsely deployed, the ability of sensors to detect occupancy change is limited by their coverage. In this way, occupancy estimation largely depends on the existing sensor technologies.

Occupancy estimation aims to adaptively correct noise and lack of observability errors by subdividing the approach into two sub-problems [37]:

i) *modelling*, investigates how to build a model to utilize prior knowledge and to simulate the occupants' movement behaviors in the building;

ii) *estimation*, defined as the process to obtain the state of a system given a model and incomplete observational data.

In SAFESENS, the modelling follows the spatial topology of the floor, as in [38], where each graph node is considered a state. It can assume either an *occupancy state*, related to any zone of the building, or a *flow state*, which reflects the uncertainty in how people move from zone to zone. This modelling permits to divide the building into non-overlapping zones, defined by a hierarchy of different spatial scales, namely floor-level, zone-level and room-level.

However, in our approach, we defined two new graph-based models, thus having the following ones: i) *G-node*, which only includes the *occupancy* nodes and consider the exits as *flow* nodes; ii) *G-flow*, as the previous ones but also incorporates a *flow* node between *occupancy* nodes that are connected, in order to represent their transitions; iii) *G-biflow*, which adds one more *flow* node for each transition, in this way, explicitly representing the probability of flow on both directions. *G-flow* represents the baseline proposed in [38].

For the estimation, a Kalman filter (KF) framework is adopted. Due to the non-linearity of the underlying data (pedestrian behavior) and the adopted linear modelling approach, we study the performance of linear and non-linear Kalman estimators, such as Ensemble KF (EnKF), bank-of-filters-based (IMM, MMAE), among others [39].

VIII. Results

The SAFESENS component systems and subsystems were evaluated through a series of experiments to evaluate their capabilities and validate the data sets being generated.

A. Data Visualisation on the Smart App

To validate our system and to do more real life experiments, we have installed a demo of the SAFESENS localization platform at TNI near the canteen area. Under heavy NLOS and with limited available anchor nodes, the system can achieve 0.5m accuracy. Figure 5 shows the visualization front end for the SAFESENS system. In operation, it is envisaged that this user interface would be utilized by the control unit manager who would be in a position to communicate occupancy estimations dynamically to the rescue team.



Figure 5. Occupancy and Firefighter Data Visualisation.

B. Location Tracking and Activity Monitoring

The positioning and tracking performance of the module has been evaluated. An additional calibration step was added to account for antenna delay and to improve ranging performance. The experiments and results for the calibration are discussed below. The experiments comprise of an evaluation of the mobile performance employing a Least Square Estimation (LSE) algorithm, discussed in the next section along with the performance evaluation.

2018, © Copyright by authors, Published under agreement with IARIA - www.iaria.org

i. Ranging Characterisation and Calibration:

We performed ranging tests with each SAFESENS board under the same conditions. These tests were performed on all the boards before and after the antenna calibration.

For the tests, we have used one static tag and one anchor (AN) at the time. The distance between the tag/anchor was set to 238.5 cm (±0.5 cm). Each AN was connected to a Raspberry Pi (RPi), which was itself connected to a server. The RPi is used to report the ranging data, which is stored in the database on the Tyndall server for processing and analysis. The ranging results have been recorded for each board individually.

Table I reports statistical analysis for the same number of samples (265 samples) based on the average results between ranging data recorded for four boards, before and after the antenna calibration. Note that the boards that were not used in the two experiments and the faulty boards were discarded for the consistency of the experiment and the results comparison. The team embarked on a calibration exercise to eliminate thermal noise from the antenna interfaces circuitry and to calibrate each antenna individually. The experiment was carried out again following the same procedure using these calibrated systems.

From these results, we noticed the improvement that was brought by the antenna calibration. The ranging errors have dropped by 55.81 cm on average, which is quite significant for our application.

TABLE I. STATISTICAL RESULTS FOR RANGING CHARACTERISATION

	AVG Results Before the Calibration	AVG Results After the Calibration
MAX Ranging Distance (cm)	347.75	259.25
MIN Ranging Distance (cm)	299	249.75
AVG Ranging Distance (cm)	311.76	255.95
STD Ranging (cm)	60.5	2.2185
MAX Ranging Error (cm)	109.25	16.64
MIN Ranging Error (cm)	60.5	1.86
AVG Ranging Error (cm)	73.260	17.45

ii. Localization Algorithm:

For our localization algorithm, we have considered a real-case scenario in a 2D plane with 8 calibrated anchors (ANs) set at known positions (x_i, y_i), with $i = 1,2,\dots,8$ and used one mobile node (MN) for the tracking with coordinates (x_e, y_e). Using the Time of Arrival (TOA) information, we can calculate the estimated distances r_i at each AN:

$$\boldsymbol{r_i = c \cdot \bar{\tau}_i = d_i + b_i + n_i},$$

where, c is the speed of light, $\bar{\tau}_i$ is the measured TOA information at i^{th} AN, b_i is the Non-line-of-sight (NLOS) bias for the i^{th} measured distance, n_i is the noise at the i^{th} measured distance, and d_i is the real distance between the i^{th} AN and the MN This distance is defined as follows:

$$\boldsymbol{d_i = \sqrt{(x_i - x_e)^2 + (y_i - y_e)^2}},$$

The system described by the equations above can be solved to find the unknown (x_e, y_e) coordinates of the MN, based on the LSE method. The LSE is known to be the most popular algorithm for positioning computation due to its' low complexity computation [6].

The LSE is based on the following estimation function:

$$(\boldsymbol{x_e, y_e}) = \boldsymbol{arg \min_{x_e, y_e}\{R(x_e, y_e)\}}$$

$$= \boldsymbol{arg \min_{x_e, y_e}\left\{\sum_{i=1}^{N}(r_i - \|(x_e, y_e) - (x_i, y_i)\|)^2\right\}},$$

where $R(x_e, y_e)$ is the residual error of $\boldsymbol{r_i}$ *and* $\|(x_e, y_e) - (x_i, y_i)\|$. This equation has been implemented in our localization engine in the server and used for the computation of the localization of the MN.

The formulation for location estimation is given by:

$$\begin{bmatrix} x_e \\ y_e \end{bmatrix} = (P^T P)^{-1} P^T B$$

where:

$$\begin{bmatrix} x_2 & y_2 \\ x_3 & y_3 \\ \vdots & \vdots \\ x_n & y_n \end{bmatrix} = P \text{ and } \frac{1}{2}\begin{bmatrix} (x_2^2 + y_2^2) - r_2^2 + r_1^2 \\ (x_3^2 + y_3^2) - r_3^2 + r_1^2 \\ \vdots \\ (x_n^2 + y_n^2) - r_n^2 + r_1^2 \end{bmatrix} = B$$

iii. Performance Evaluation and Discussion:

To evaluate the performance of our tracking platform, practical tests were carried out at the TNI. Results before and after calibration are illustrated in Figures 6 and 7, respectively. For each experiment, a reference path (shown in the figures below in blue) was determined for the mobile subject and communicated via markers on the floor. The tag was instrumented on the arm of the subject, who subsequently simulated the emergency responder walking along the reference path. The green path illustrates the calculated trajectory of the subject employing the module. The results indicate that the tolerances are acceptable for the prescribed application. Results for the activity classification machine learning algorithms are presented in [40].

From the two presented Figures 6 and 7 below, we can say that the calibration has also significantly enhanced the ranging and thus the positioning/tracking accuracies.

2018, © Copyright by authors, Published under agreement with IARIA - www.iaria.org

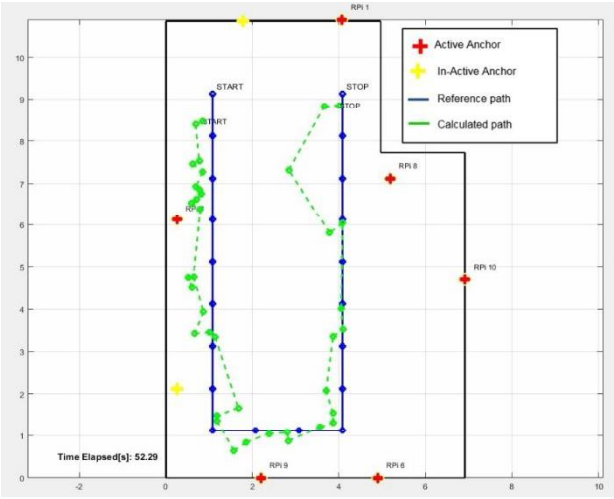


Figure 6. SAFESENS hybrid inertial, positional and navigation module mobile tracking performance prior to calibration

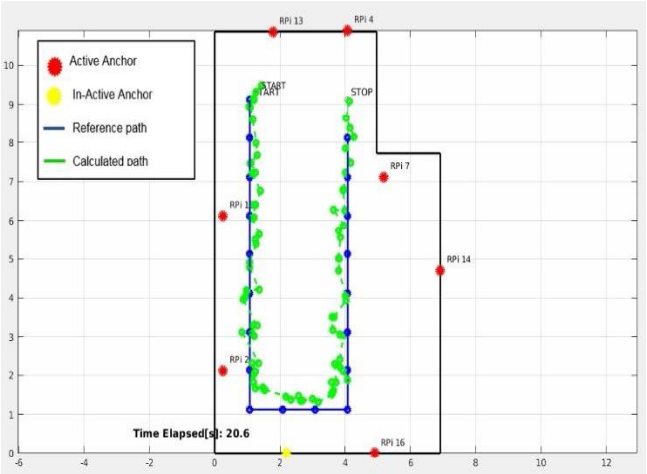


Figure 7. SAFESENS hybrid inertial, positional and navigation module mobile tracking performance following calibration

C. *Vital Signs*

The vital signs monitor is implemented as a finger ring embedded in the firefighter glove. It can operate in two different modes; high-resolution heart-rate, or combined heart-rate and blood oxygenation.

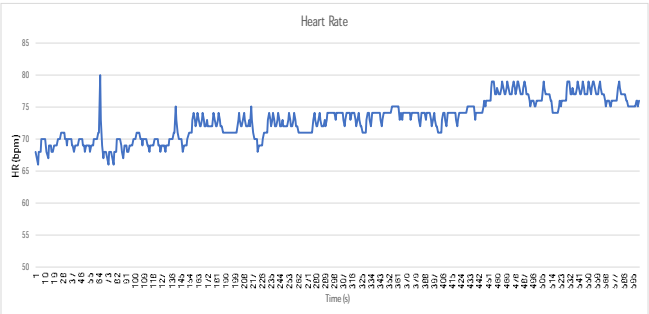


Figure 8. Evolution of heart rate over a period of 10 minutes.

The heart rate does not require multiple wavelengths, and thus a more optimal LED firing pattern can be selected to either lower the total power consumption or increase the sampling rate. Figure 8. shows an example of the heart rate captured over a period of ten minutes.

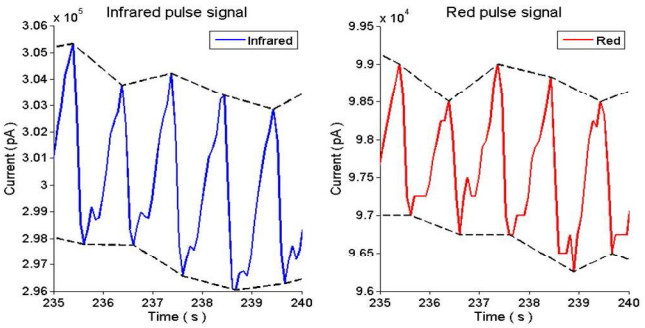


Figure 9. Captured infrared and red PPG signals.

Estimation of the blood oxygenation requires alternate firing of red and IR LEDs, and a more complex algorithm. An example of the captured data is shown in Figure 9.

The PEFAC algorithm [41] was selected for the heart rate detection. This method estimates the heart rate from the frequency spectrum. By expressing the frequency in the log-domain, the distance between the fundamental frequency and its harmonics doesn't depend on the absolute value of the fundamental frequency. By convolving the spectrum with a matched filter, the spectra of the harmonics are accumulated and noise is rejected. The oxygen saturation (SpO_2) is then derived from the ratio of ratios R, which is defined by:

$$R = \frac{(AC/DC)_1}{(AC/DC)_2}$$

where AC and DC are the peak-to-peak amplitude and the baseline of the PPG pulse, respectively. These values are found by applying a min/max envelope tracker on the cleaned PPG signal. The following relationship between the ratio R and the SpO_2 is then used:

$$SpO_2 = \frac{\varepsilon_{d1} - R(I_2/I_1)\varepsilon_{d2}}{R\left(\frac{I_2}{I_1}\right)(\varepsilon_{o2} - \varepsilon_{d2}) + (\varepsilon_{d1} - \varepsilon_{o1})}$$

where ε_o and ε_d are the extinction coefficients for HbO_2 (oxyhemoglobin) and Hb (hemoglobin). The constants l_1 and l_2 are the path-lengths for the two wavelengths and depend strongly on the scattering coefficient. For the two wavelengths in the red and infrared regions, which are used in the glove ring sensor (IR 950nm and red 660nm), l_1 and l_2 are expected to differ and they are unknown. SpO_2 can be derived from R through the calibration process by assuming that l_2/l_1 is a constant that is independent of inter-subject variability in the circulatory system. In this case, the coefficients are constants and can be determined through calibration. If the parameter

2018, © Copyright by authors, Published under agreement with IARIA - www.iaria.org

I_2/I_1 changes between different subjects, in particular between the healthy subjects on whose fingers the calibration was performed and the fireman wearing the glove, inaccuracy in the SpO_2 measurement is to be expected. Relative changes for a single subject are accurate.

i. Flammable Gas Sensing

The hydrogen sensor was evaluated using humidified synthetic air with different amounts of H_2 added, in the range from 0.02% to 2% volume concentration. The gas was fed to the sensor with a nozzle with a flow of 1slm (standard liter per minute). The sensor chip was externally heated to temperatures of up to 140°C. It was found that 0.02% concentration already results in a detectable sensor signal. For concentrations above 0.5%, saturation of the signal began to be observed. Response time t_{90} was found to be in the range of 100s. Further reduction of response time is to be achieved by using PLD (Pulsed Laser Deposition) in order to generate a porous Pd-Ni layer, facilitating the H_2 transport into the layer.

The methane sensor was evaluated in a gas mixing chamber, where gas flows of methane were mixed with compressed dry air. Initial experiments consisted of cyclic voltammetry, where the voltage of the sensor is scanned to observe at which voltage the largest effect of methane exposure is observed.

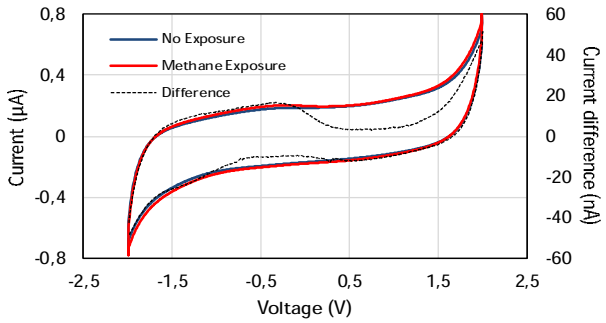


Figure 10. Cyclic voltammetry to determine most suitable voltage level for methane detection. The difference between the current levels is plotted with the dotted line, and should be evaluated on the right Y-axis.

In Figure 10, the cyclic voltammogram of the sensor with and without 5% methane exposure is plotted. The difference between the observed currents is small compared to the background current. To make the difference more visible, the currents with and without methane exposure were subtracted, and plotted. From these plots it becomes clear that the largest current difference is observed between -0.5 and -1.5 V. The extreme voltages near -2 and +2 V are excluded, because water electrolysis will occur at these voltages when measurements are performed in humid air, which will interfere with the detection of methane.

To determine the response of the sensor, the voltage was fixed, and the current was used as an indicator of the methane exposure. In Figure 11, the current that is resulting of 5% methane is given. This figure shows that the sensor has a fast response time, and that the gas level can already be detected within a few seconds, which is crucial for first responders.

.

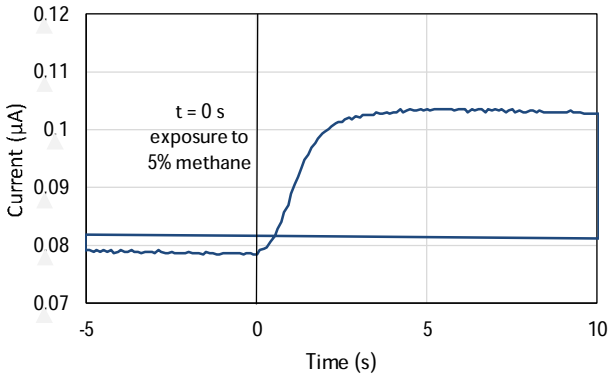


Figure 11. Current response to an exposure of 5% methane

First responders often need to work in extreme conditions where temperatures may reach high levels. For the hydrogen sensor, this may only have a limited influence, since this sensor is heated using an internal heat source. The methane sensor is, however, operating at ambient temperature and may be influenced by temperature changes due to these environments in which first responders operate, as shown in Figure 12.

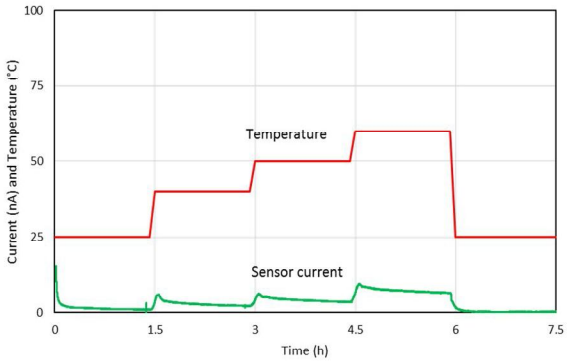


Figure 12. Temperature influence on the sensor background current. In red, the temperature profile setting is displayed, while the green line shows the measured sensor response.

To test the temperature influence, the sensor was placed in a climate chamber, and the changes in the background current related to temperature increases was evaluated. The temperature was increased stepwise, starting at 25 °C, and held stable for 1.5 h at 40, 50 and 60 °C. Results for this measurement are plotted in Figure 12. In this figure, it can be clearly observed that there is an influence of the temperature on the background current. The characteristic step profile of the temperature comes back in the measured current. It can, however, also be seen that the temperature influence is transient, and that the initial current response to temperature changes is stronger than the equilibrium response.

Most important, however, is the observation that, when the current response to temperature changes up to 60 degrees is compared to the current response to methane, that the current is only increased by less than 10 nA, while the response to relevant concentrations of methane is much stronger. From

2018, © Copyright by authors, Published under agreement with IARIA - www.iaria.org

this observation it can therefore be concluded that the developed methane sensor can be used in these high temperature conditions. It's accuracy will benefit from temperature compensation, which will require input from a separate temperature sensor, but this is not crucial.

D. Occupancy Detection

The deployment scenario is very particular since it depends on the physical venue, the sensor network characteristics and the application domain. Therefore, the solutions will perform very differently from scenario to scenario. For these reasons, the conducted experiments consider the combination of three characteristics: i) physical layout; ii) sensor topology; iii) data modelling (e.g., synthetic-random, synthetic- pedestrian; real sensors), as in Table II.

TABLE II. EVALUATION METRICS FOR EACH ESTIMATOR, CONSIDERING THE *G-FLOW* MODELLING APPROACH, FOR T = 90000 SAMPLES

Estimator	Topology	MSE	Precision	Recall	F-measure
KF	TA	1.445	99.81	53.85	69.96
	TB	0.665	99.88	68.42	81.21
EnKF	TA	1.734	93.74	51.51	66.49
	TB	1.003	97.42	56.47	71.50
HF	TA	1.553	99.88	49.67	66.61
	TB	1.554	99.88	49.94	66.59
IF	TA	2.826	99.56	49.36	66.01
	TB	1.482	99.60	50.95	67.41
UKF	TA	1.373	99.37	54.76	70.61
	TB	0.657	99.88	68.44	81.22
IMM	TA	1.384	99.86	53.76	69.90
	TB	0.781	97.60	63.81	77.17
MMAE	TA	1.423	99.81	53.92	70.01
	TB	0.664	99.88	68.42	81.22

Due to space constraints, we here only present the results for selected estimators and for one tested scenario, which consists of 6 rooms, with two different sensor topologies: TA) two camera sensors with oblique view towards ground-floor, situated in two rooms, and a camera sensor with top-down view, positioned between two rooms; TB) camera sensor in each room and the same top-down view camera between two rooms.

The data was simulated using the Helbing social force model [42], rules for interactions between occupants and obstacle avoidance awareness. The simulation considers a total occupancy up to 6 people during 9000 samples (approximately lasting 7.5 minutes). As expected, having a sensor in every zone dramatically improves the overall estimation. Considering all the experiments, we verified that the linear estimators are preferred for local measurements but they show degradation of performance through time as well as for global estimation.

An interesting conclusion is that a bank of linear filters solutions show competitive results, which might open further investigation issues regarding their extension to the combination of linear and non-linear estimators to balance local with global estimation.

Many experiments were also conducted in the Tyndall scenario, with real information captured from the sensor-network, in order to fully validate the occupancy detection system. Table III shows the results from all the states of the graphs, considering the average taken from the months of August and September 2017.

The most important conclusions that can be taken from the analysis of the estimators' performance in both the simulated and real scenarios shown in Table III are: i) *G-node* presents the best performance in most of the estimators. Its' recall is always the higher one, which shows its' relevance to estimate the real number of occupants in the entire floor; ii) the bank of filters approaches is revealed to be the most accurate for global estimation; iii) *G-flow* presents lower MSE than the sensors-only readings, proving their superior local performance in the zones with sensors; iv) *G-biflow* performs better when the sensors are located within the zones, while G-node behaves better when the sensors are placed in regions of transition between zones.

TABLE III. EVALUATION METRICS FOR EACH ESTIMATOR CONSIDERING THE AVERAGE TAKEN FROM THE MONTHS OF AUGUST AND SEPTEMBER 2017, AND THE THREE GRAPH-BASED MODELS, {G-NODE, G-FLOW, G-BIFLOW}

Period Aug./Sept. 2017	MSE			Precision			Recall			F-measure		
	G-node	G-flow	G-biflow	G-node	G-flow	G-biflow	G-node	G-flow	G-biflow	G-node	G-flow	G-biflow
KF	**25.78**	27.01	45.16	80.04	84.99	**86.39**	52.47	**62.90**	49.87	63.09	**72.00**	62.98
EKF	25.78	**24.90**	31.31	79.94	84.84	**87.50**	52.50	**64.02**	60.50	63.08	**72.71**	71.36
UKF	**25.90**	27.05	45.16	80.27	85.03	**86.38**	52.40	**62.86**	49.87	63.11	**72.00**	62.97
EnKF	**27.16**	41.02	55.29	80.43	77.44	**82.46**	52.00	**56.66**	50.00	62.82	**65.16**	62.12
CKF	**25.90**	27.05	45.16	80.27	85.02	**86.38**	52.40	**62.86**	49.87	63.11	**71.99**	62.97
HF	**30.11**	100.1	85.97	81.71	**84.76**	81.58	51.15	**52.77**	51.54	62.56	**64.74**	62.95
IMM	**22.76**	25.26	48.52	79.48	84.73	**87.09**	53.46	**63.69**	47.43	63.66	**72.39**	61.04
MMAE	**18.92**	47.46	67.04	80.65	82.48	**87.68**	57.46	**60.88**	52.85	66.63	**69.63**	65.64

2018, © Copyright by authors, Published under agreement with IARIA - www.iaria.org

IX. Conclusions and Future Work

The SAFESENS system is currently deployed in the Tyndall National Institute in Cork, Ireland where the integration activity focuses on the occupancy detection and firefighter activity tracking [1]. The deployment activity continues to progress so as to integrate datasets from the other sensors integrated in the system, to improve accuracy of the sensor readings and develop robust communications to augment the infrastructure based communications currently used in the demonstration activity, which is Wi-Fi based. This will focus on UWB based Media Access Control (MAC), routing and scheduling protocols to maximize energy efficiency and minimize system latencies. The smartphone application is being developed to integrate data sets from all sensors for upload to the server for analytics and visualisation.

For first responder tracking, by using the LSE algorithm and performing the calibration, we have significantly enhanced the ranging and improved the positioning/tracking accuracy for real time positional information acquisition. However, there is still room for improvement in the accuracy of the algorithm, in terms of precision. Although the LSE algorithm has shown good results in LOS environment, it remains very sensitive to heavy NLOS conditions. Error mitigation techniques, before the computation of the localization, will have a good impact on achieving a better tracking accuracy. The requirement for a number of anchor nodes for the localization will need to be addressed, and the ability for the localization tags to use each other as mobile anchor nodes referenced to a known coordinate is envisaged. This work is the subject of our future research in this area.

A glove with an optical sensor to measure the wearer's heart rate has been accomplished by using a soft and stretchable circuit board based on thermoplastic elastomers. First measurements are indicating the good data quality and mechanical robustness of the textile-integrated electronic system. Future investigations will be conducted in order to explore the limit of possible bending and folding loads and to determine the long term reliability of the stretchable electronics. A SAFESENS heart rate monitor has been integrated into this fire-retardant glove to give real time physiological information over Bluetooth.

Electrochemical explosive/flammable gas detectors have been developed, which are sensitive to methane at a range of operational temperatures – such as those experienced by first responders, with a fast response time in the order of seconds. Future work will address further the speed of response of the explosive gas sensors.

For the most precise measurement of occupancy levels within the built environment, we can make the following observations: G-biflow performs better when the sensors are located within the zones whereas G-node performs better when the sensors are placed in the regions of transition between zones. The graph model G-node presents the best performance in most of the estimators. Its' recall is always the higher one, which shows its' relevance to estimate the real number of occupants in the entire floor. The bank of filters approaches is the most accurate for global estimation and better temporal adaptation. The graph model G-flow presents lower MSE than the sensors-only readings, proving their superior local performance in the zones with sensors. In general, for accurate occupancy measurement, the observability of the sensors in the whole sensor topology is crucial to ensure a reliable global performance of the occupancy estimation.

Acknowledgment

This work is supported by ENIAC-JU-2013-1(621272), via the SAFESENS project (Sensor Technologies for Enhanced Safety and Security of Buildings and its Occupants).

The authors would like to acknowledge the support of National funding agencies including Enterprise Ireland. This publication has emanated from research supported in part by a research grant from Science Foundation Ireland (SFI) and is co-funded under the European Regional Development Fund under Grant Number 13/RC/2077.

References

[1] B. O'Flynn et al., "SAFESENS – Smart Sensors for Fire Safety First Responders Occupancy, Activity and Vital Signs Monitoring", In Proc. The Eleventh International Conference on Sensor Technologies and Applications, (SENSORCOMM 2017), Rome, Italy, 10-14 Sept, 2017.

[2] S. Tedesco, J. Khodjaev, and B. O'Flynn, "A novel first responders location tracking system: Architecture and functional requirements", Proc. IEEE 15th Mediterranean,Microwave Symposium (MMS 2015), IEEE Press, Nov. 2015, pp. 1-4.

[3] M. Walsh, S. Tedesco, T. Ye, and B. O'Flynn, "A wearable hybrid IEEE 802.15. 4-2011 ultra-wideband/inertial sensor platform for ambulatory tracking", Proceedings of the 9th International Conference on Body Area Networks, ICST (Institute for Computer Sciences, Social-Informatics and Telecommunications Engineering), 2014, pp. 352-357.

[4] http://www.equivital.co.uk/assets/common/SEM_Data_Sheet_General_HIDA3330-DSG-02.2_.2_.pdf (Accesssed 30/05/2018)

[5] http://phaser.med.ucla.edu/ (Accesssed 30/05/2018)

[6] http://globeturnoutgear.com/innovation/wasp (Accesssed 30/05/2018)

[7] A. Cavanaugh, M. Lowe, D. Cyganski, and R. J. Duckworth, "A new Bidirectional Transaction Approach to Improve Precision Location in Indoor Environments," in Proceedings of the Institute of Navigation International Technical Meeting, (San Diego, California), January 2011

[8] https://www.draeger.com/en-us_us/Fire-Services/Productselector/Mobile-Gas-Detection (Accesssed 30/05/2018)

[9] https://www.scottsafety.com/en-gb/ (Accesssed 30/05/2018)

[10] https://www.ionscience.com/ (Accesssed 30/05/2018)

[11] http://www.rkiinstruments.com/product-category/portable-gas-monitors/multi-gas-monitors/ (Accesssed 30/05/2018)

[12] https://www.raesystems.com/solutions/sensors (Accesssed 30/05/2018)

[13] http://www.navsys.com/products/poscomm.htm (Accesssed 30/05/2018)

[14] http://www.seertechnology.com/naviseer (Accesssed 30/05/2018)

[15] http://www.wmscom.com/index.php?q=about-us/news/harris-gr-100-delivering-accurate-first-responder-information-incident-commanders-and- (Accesssed 30/05/2018)

2018, © Copyright by authors, Published under agreement with IARIA - www.iaria.org

[16] http://www.ensco.com/products-services/gps-denied-geolocation-navigation/personnel-navigation.htm (Accesssed 30/05/2018)

[17] http://www.trxsystems.com/trx-systems-blog/bid/48872/Sentrix-GPS-Denied-Tracking-Now-Commercially-Available (Accesssed 30/05/2018)

[18] http://www.honeywellnow.com/2012/04/26/honeywell-tests-glanser-system-to-locate-and-track-firefighters/ (Accesssed 30/05/2018)

[19] http://blog.al.com/huntsville-times-business/2010/08/q-track_has_a_successful_launc.html (Accesssed 30/05/2018)

[20] http://www.robot.uji.es/documents/rise08/reports/Harmer.pdf (Accesssed 30/05/2018)

[21] https://tetradev.motorolasolutions.com/Extranet/GettingStarted.aspx (Accesssed 30/05/2018)

[22] T. Ye, M. Walsh, P. Haigh, J. Barton, and B. O'Flynn, "Experimental impulse radio IEEE 802.15. 4a UWB based wireless sensor localization technology: Characterization, reliability and ranging", Proc. 22nd IET Irish Signals and Systems Conference, (ISSC 2011), Dublin, Ireland. 23-24 June 2011.

[23] N. N. Brushlinsky, M. Ahrens, S. V. Sokolov, and P. Wagner, World Fire Statistics. Technical report 21. Center of Fire Statistics, International Association of Fire and Rescue Services, 2016. [Online] Available from: http://www.ctif.org/ctif/world-fire-statistics (Accesssed 30/05/2018)

[24] J. Khodjaev, P. Yongwan, and A. S. Malik, "Survey of NLOS identification and error mitigation problems in UWB-based positioning algorithms for dense environments", annals of telecommunications-annales des télécommunications 65, no. 5-6, pp. 301-311, 2010.

[25] J. Khodjaev, S. Tedesco, and B. O'Flynn, "Improved NLOS Error Mitigation Based on LTS Algorithm", Progress In Electromagnetics Research Letters 58, pp. 133-139, 2016.

[26] J. Khodjaev, A. Narzullaev, Y. Park, W. Jung, J. Lee, and S. Kim, "Performance Improvement of Asynchronous UWB Position Location Algorithm Using Multiple Pulse Transmission," Proc. 4th Workshop on Positioning, Navigation and Communication, 2007. (WPNC'07), IEEE, 2007, pp. 167-170.

[27] Y. M. Chi, T. P. Jung, and G. Cauwenberghs, "Dry-Contact and Noncontact Biopotential Electrodes: Methodological Review," in IEEE Reviews in Biomedical Engineering, vol. 3, pp. 106-119, 2010.

[28] S. Sudin et al., "Wearable heart rate monitor using photoplethysmography for motion," 2014 IEEE Conference on Biomedical Engineering and Sciences (IECBES), Kuala Lumpur, 2014, pp. 1015-1018.

[29] D. Damianou, "The Wavelength Dependence of the Photoplethysmogram and its Implication to Pulse Oximetry", PhD Thesis, University of Nottingham, October, 1995.

[30] M. Gonzales, F. Axisa, F. Bossuyt, Y. Hsu, B. Vandevelde, and J. Vanfleteren, "Design and Performance of Metal Conductors for Stretchable Electronic Circuits", Proc. of the ESTC 2008, London, September 2008, pp. 1-4.

[31] T. Loher et al., "Stretchable electronic systems," 2006 8th Electronics Packaging Technology Conference, Singapore, 2006, pp. 271-276.

[32] R. Vieroth, T. Loeher, M. Seckel, C. Dils, C. Kallmayer, A. Ostmann, and H. Reichl, "Stretchable Circuit Board Technology and Application," 2009 International Symposium on Wearable Computers, Linz, 2009, pp. 33-36.

[33] M. A. G. Zevenbergen, D. Wouters, V.-A. T. Dam, S. H. Brongersma, and M. Crego-Calama, "Electrochemical Sensing of Ethylene Employing a Thin Ionic-Liquid Layer", Analytical Chemistry, vol. 83, pp. 6300-6307. 2011.

[34] J.F.M. Oudenhoven, W. Knoben, and R. van Schaijk, "Electrochemical Detection of Ammonia Using a Thin Ionic Liquid Film as the Electrolyte", Procedia Engineering, vol. 120, pp. 983-986, 2015.

[35] R. C. Hughes and W. K. Schubert, "Thin films of Pd/Ni alloys for detection of high hydrogen concentrations", J. Appl. Phys. vol. 71, iss. 1, pp. 542-544, 1992.

[36] Z. Wang, M. Guo, G. Baker, J. R. Stetter, L. Lin, A. J. Mason, and X. Zeng, "Methane–oxygen electrochemical coupling in an ionic liquid: a robust sensor for simultaneous quantification", Analyst, vol. 139, iss. 20, pp. 5140-5147, 2014.

[37] H. T. Wang, Q. S. Jia, C. Song, R. Yuan, and X Guan, "Estimation of occupancy level in indoor environment based on heterogeneous information fusion", Proc. 49th IEEE Conference on Decision and Control (CDC 2010). IEEE. Dec. 2010, pp. 5086-5091.

[38] R. Tomastik, S. Narayanan, A. Banaszuk, and S. Meyn, "Model-based real-time estimation of building occupancy during emergency egress", In Pedestrian and Evacuation Dynamics 2008, W. Klingsch, C. Rogsch, A. Schadschneider, M. Schreckenberg, Eds Springer Berlin Heidelberg. pp. 215-224, 2010.

[39] L. Houtekamer and H. L. Mitchell, "Ensemble kalman filtering". In: Quarterly Journal of the Royal Meteorological Society, 131(613), pp. 3269-3289, 2005.

[40] S. Scheurer, S. Tedesco, K. N. Brown, and B. O'Flynn, "Human Activity Recognition for Emergency First Responders via Body-Worn Inertial Sensors", Proc. 14th International Conference on Wearable and Implantable Body Sensor Networks, (BSN'17), Eindhoven, The Netherlands, May 9-12, 2017.

[41] S. Gonzalez and M. Brookes, "PEFAC-a pitch estimation algorithm robust to high levels of noise," IEEE/ACM Transactions on Audio, Speech, and Language Processing, vol 22, issue 2, pp. 518-530, 2014.

[42] D. Helbing and P. Molnar, "Social force model for pedestrian dynamics", Physical review E, 51(5), pp. 4282-4286, 1995.

2018, © Copyright by authors, Published under agreement with IARIA - www.iaria.org